

Chiral separation and modeling of the three-chiral-center β -blocker drug nadolol by simulated moving bed chromatography

Xin Wang*, Chi Bun Ching

Chemical and Process Engineering Centre (CPEC), National University of Singapore, Block E5 Basement 08,
4 Engineering Drive 4, Singapore 117576, Singapore

Received 16 September 2003; received in revised form 17 February 2004; accepted 17 February 2004

Abstract

Nadolol, a β -blocker used in the management of hypertension and angina pectoris, has three chiral centers and is currently marketed as an equal mixture of its four stereoisomers. Resolution of three of the four stereoisomers of nadolol was obtained previously by HPLC, with a complete separation of the most active enantiomer (*RSR*)-nadolol, on a column packed with perphenyl carbamoylated β -cyclodextrin (β -CD) immobilized onto silica gel. In this study, continuous separation of the target enantiomer of (*RSR*)-nadolol from its racemic mixture (which is a ternary mixture in the chromatographic system) was studied by non-linear SMB chromatography. Different regions of (2, 3) and (1, 2) complete separation regime were determined in the (m_2 , m_3) region and the effect of non-linearity such as overall feed concentration and component composition on the separation performances was investigated. A direct simulation approach has been proposed to simulate the SMB separation performance for the pseudo-binary mixture of nadolol. The simulation was conducted on the basis of a shortcut method constituted only of the weak-key and strong-key components. The performance of the cyclic steady-state behavior of the SMB unit was predicted reasonably well. It was also discussed quantitatively that the complete separation region obtained from the shortcut method is a subset of the true complete separation region and the optimal separation conditions obtained differed slightly from the “true” separation.

© 2004 Elsevier B.V. All rights reserved.

Keywords: Enantiomer separation; Simulated moving beds; Nadolol; β -Cyclodextrin

1. Introduction

The chirality of drugs is an important issue from the pharmacological, pharmacokinetic, toxicological and regulatory points of view [1,2]. Nowadays, more research efforts have been concentrated on the production of enantiomerically pure products due to increasing demand that such drugs are administered in optically pure form [3]. Nadolol, 5-{3-[(1,1-dimethylethyl)amino]-2-hydroxypropoxy}-1,2,3,4-tetrahydro-*cis*-2,3-naphthalenediol is a β -blocker drug widely used in the management of hypertension and angina pectoris. Its chemical structure has three stereogenic centers which allows for eight possible stereoisomers. However, the two-hydroxyl substituents on the cyclohexane ring are fixed in the *cis*-configuration which precludes four stereoisomers. Nadolol is currently marketed as an equal mixture of the four

stereoisomers, designated as the diastereomers of “racemate A” and “racemate B”, as shown in Fig. 1. Racemate A is a mixture of the most active stereoisomer I ((*RSR*)-nadolol) and its enantiomer II ((*SRS*)-nadolol) in 1:1 molar ratio, whereas racemate B is a mixture of stereoisomer III ((*RRS*)-nadolol) and its enantiomer IV ((*SSR*)-nadolol) also in 1:1 molar ratio. For a safer and more effective use, it is better to separate the enantiomer (*RSR*)-nadolol before use.

Simulated moving bed (SMB) process has been extensively applied to the separation of chiral drugs and intermediates [4–7] over the last decade. Due to continuous counter-current contact between liquid and solid phases, SMB process allows the decrease of desorbent requirement and the improvement of productivity per unit time and unit mass of stationary phase. Furthermore, SMB process is believed to be able to achieve high-purity separation performance even when the resolution exhibited by an individual column is not efficient for a batch preparative process, which is often encountered in chiral separations. When applied in chiral separations, four-section (or zone) SMB has

* Corresponding author. Tel.: +65-6874-2196; fax: +65-6873-1994.
E-mail address: cpewx@nus.edu.sg (X. Wang).

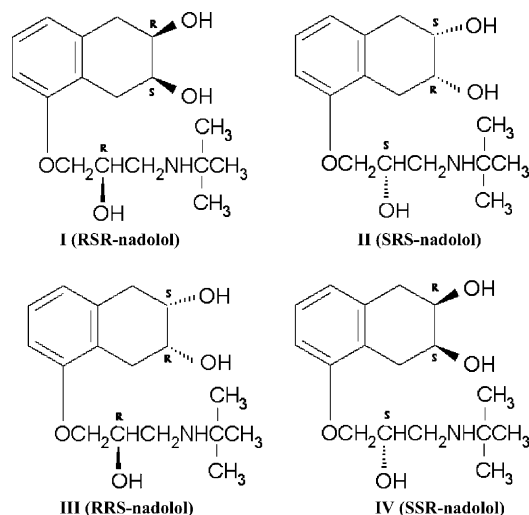


Fig. 1. Chemical structures of stereoisomers of nadolol. I (*RSR*-nadolol, SQ12148) and II (*SRS*-nadolol, SQ12150) constitute nadolol racemate A; III (*RRS*-nadolol, SQ12149) and IV (*SSR*-nadolol, SQ12151) constitute nadolol racemate B.

been widely applied in binary separation of one chiral center racemates. Besides binary mixtures, four-section SMB can also be used to divide multi-component mixtures into strong adsorbing and weak adsorbing fractions [8,9] and is able to produce pure product if the target compound belongs to the most (or least) retained species in the ternary mixture. More recently, to overcome the limitations of SMB process, namely separation of binary mixtures or recovery of one component from a multi-component mixture, modeling and parametric study of a JO process for the separation of ternary mixtures by a pseudo-SMB process was presented [10]. The process, firstly developed by the Japan Organo Company [11], is divided into two steps. In particular, step 1 of the cycle is considered to be equivalent to a series of preparative chromatographic columns, where the intermediate component of the ternary mixture is produced. In step 2, similar to a simulated moving bed (SMB), there is no feed and the less adsorbed species is collected in the raffinate while the more retained species is collected in the extract. High purity and recovery of all three components could be achieved by this process [12].

For β -blocker drug nadolol, resolution of three of its four stereoisomers was obtained by HPLC in a previous study [13]. A complete separation of the most active enantiomer (*RSR*)-nadolol was achieved on the column packed with perphenyl carbamoylated β -cyclodextrin (β -CD) immobilized onto silica gel. Since the target enantiomer of (*RSR*)-nadolol is the most retained component in our chromatographic system, four-zone SMB is therefore capable of separating this enantiomer from its ternary mixture. Different separation regimes of (2, 3) and (1, 2) complete separation were examined and the effect of non-linearity such as the overall feed concentration and component composition on the separation performances was investigated. A practical way

of obtaining the approximate optimal operation condition from experimental results was also proposed. Lastly, modeling and simulation of the pseudo-binary separation was performed on the basis of a shortcut method.

2. Theoretical

2.1. Complete SMB separation for multi-component system

In the frame of equilibrium theory, which neglects mass transfer resistances and axial dispersion, true counter-current (TCC) adsorption model was employed by Storti et al. [14–16] and Mazzotti et al. [8,17,18] in a series of efforts to obtain explicit expressions of the fluid to solid flow rate ratios, m_j ($j = 1, \dots, 4$), for complete separation of binary mixtures. The operation condition of SMB was then determined based on the equivalence between SMB and TCC process. In special, desorbent is usually non-adsorbable (or it is so weak that its adsorptivity is negligible) for enantiomeric separation, and explicit criteria were obtained [19] to determine the boundaries of the complete separation region in the space spanned by m_j ($j = 1, \dots, 4$).

The four-zone SMB can be applied for multi-component two-fraction separations and pure product can be produced if the target compound belongs to the most (or least) retained species. The (n, p) separation regime of a C -component system is defined as the one where the less retained components labeled from 1 to n are collected in the raffinate, and the more retained species, with indices from p to C , are collected in the extract. For a complete (n, p) separation, $p = n + 1$ and no component distributes between raffinate and extract streams. For a multi-component system with a desorbent having any adsorptivity, the complete separation region could be determined by trial and error method [8]. Recently, complete separation regions for a system constituted of an inert solvent and C solutes, which interact with the stationary phase according to non-stoichiometric Langmuir model, were determined by using ω -transformation [9]. In this method, introduction of function T_2 was the key feature which made significant improvement over previous approaches, since it allows dealing with only two zeros of the function T_2 (ω^- , ω^+) in the interval of interest whatever the number of components to be separated. Through a one-to-one mapping between (ω^- , ω^+) and (m_2 , m_3) planes, the boundaries and coordinates of their intersection points of the (n, p) complete separation region can be established (refer to Fig. 2 for the definition of boundaries and intersection points):

$$\text{Straight line } c_n w_{n,p} : m_2 = \frac{E''(a_n, \omega)}{E'(a_n, \omega)} (\omega_p^F < \omega < a_p) \quad (1)$$

$$\text{Straight line } w_{n,p} r_{n,p} : m_2 = \frac{E''(\omega, \omega_p^F)}{E'(\omega, \omega_p^F)} (a_n < \omega < \omega_p^F) \quad (2)$$

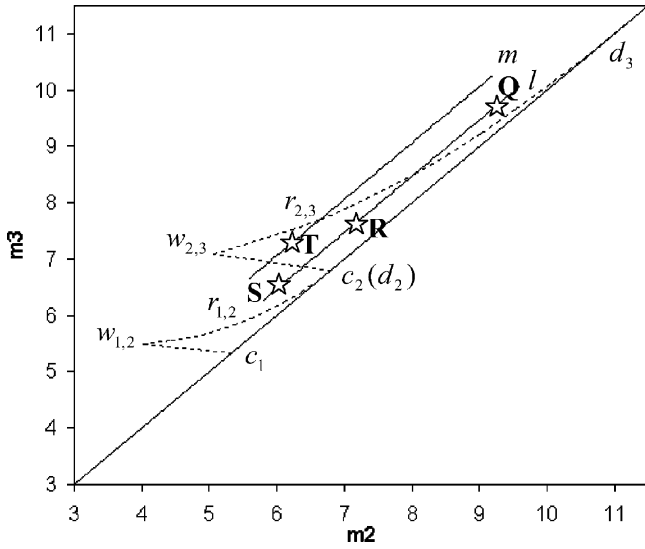


Fig. 2. Separation regions for ternary mixture of nadolol in four-zone SMB (feed concentration is 0.25 mg/min).

$$\text{Curve } r_{n,p}d_p : m_2 = \frac{E''(\omega, \omega)}{E'(\omega, \omega)} (\omega_p^F < \omega < a_p) \quad (3)$$

$$\text{Point } c_n : m_2 = m_3 = a_n \quad (4)$$

$$\text{Point } d_p : m_2 = m_3 = a_p \quad (5)$$

$$\begin{aligned} \text{Optimal point } w_{n,p} : m_2 &= \frac{E''(\omega_p^F, \omega_p^F)}{E'(\omega_p^F, \omega_p^F)}, \\ m_3 &= \frac{1 + E''(\omega_p^F, \omega_p^F)}{E'(\omega_p^F, \omega_p^F)} \end{aligned} \quad (6)$$

$$\text{Point } r_{n,p} : m_2 = \frac{E''(a_n, \omega_p^F)}{E'(a_n, \omega_p^F)}, \quad m_3 = \frac{1 + E''(a_n, \omega_p^F)}{E'(a_n, \omega_p^F)} \quad (7)$$

where function $E(\omega)$ and its first and second derivative $E'(\omega)$ and $E''(\omega)$ are expressed as:

$$E(\omega) = \sum_{i=p}^C \frac{b_i C_i^F}{a_i - \omega} \quad (8)$$

$$E'(\omega_1, \omega_2) = \sum_{i=p}^C \frac{a_i b_i C_i^F}{(a_i - \omega_1)(a_i - \omega_2)} \quad (9)$$

$$E''(\omega_1, \omega_2) = \omega_1 \omega_2 \sum_{i=p}^C \frac{b_i C_i^F}{(a_i - \omega_1)(a_i - \omega_2)} \quad (10)$$

And a_i and b_i are coefficients of Langmuir adsorption isotherm:

$$q_i^* = \frac{a_i C_i}{1 + \sum_{j=1}^n b_j C_j} \quad (11)$$

Knowing Langmuir isotherm and feed concentrations, multi-component complete separation region can be constructed in the (m_2, m_3) plane for any (n, p) separation regime. Furthermore, it is worth noting that for proper operation of SMB, adsorbent and fluid should be regenerated in sections 1 and 4, respectively, and the following constraints must be fulfilled:

$$m_1 > m_{1,cr} = a_1 \quad (12)$$

$$m_4 < m_{4,cr} \quad (13)$$

The physical meaning of Eq. (12) is that in section 1 the most retained component must be eluted from the solid phase by the eluent. In the limiting case, rear flank of the corresponding wave transition of the most retained component must be standing in section 1. In section 4, the critical condition is realized when the weakest adsorbed component shock is standing. For a complete separation, the critical value of m_4 can be determined from the following equation (noting that $m_{4,cr} = \omega_1^R$) [9]:

$$(m_3 - m_2) \frac{\omega}{m_3 - \omega} \sum_{i=1}^p \frac{b_i c_i^F}{a_i - \omega} = 1 \quad (14)$$

2.2. Operation and modeling of SMB for multi-component system

Since the equivalence between TCC and SMB units has been well established and extensively used [20], understanding and design of SMB should resort to the study of its corresponding hypothetical TCC by keeping constant the liquid velocity relative to the solid velocity in the two processes:

$$v_{L,j}^{SMB} = v_{L,j}^{TCC} + v_S \quad (15)$$

$$Q_S^{TCC} t^* = V(1 - \varepsilon) \quad (16)$$

$$Q_j^{SMB} = \left(Q_j^{TCC} + \frac{Q_S^{TCC} \varepsilon}{1 - \varepsilon} \right) \quad (17)$$

The net fluid phase flow rate over solid-phase flow rate of TCC unit can be defined as:

$$m_j = \frac{Q_j^{TCC} - Q_S \varepsilon_p}{Q_S (1 - \varepsilon_p)} \quad (18)$$

Which can be converted to the flow rate ratios of the equivalent SMB unit using the conversion rules of Eqs. (16) and (17):

$$m_j = \frac{Q_j^{SMB} t^* - V \varepsilon^*}{V(1 - \varepsilon^*)} \quad (19)$$

The parameters m_j ($j = 1, \dots, 4$) define a four-dimensional space divided into different regions, and it is useful to consider the projection of the four-dimensional regions onto (m_2, m_3) plane. The boundaries between the different separation regions depend on the multi-component adsorption

isotherm of the mixtures to be separated and feed concentration and composition. The proper values of m_2 and m_3 can be selected according to the complete (n, p) separation region and attempts should be made to increase production rate and enrichment, decrease desorbent consumption and at the same time maintain the robustness of operation. It should be noted that either switching time, t^* , or equivalently Q_1 , the largest flow rate in the unit, should be determined by taking into account the upper limit of operation pressure in the unit. Having decided m_j ($j = 1, \dots, 4$) and t^* (or Q_1), Eq. (19) is often used to determine the liquid flow rate in the four sections of SMB and thus the inlet & outlet streams flow rates. The advantage of this approach is that the flow rate ratio is a dimensionless group bringing together information about column volume, V , unit flow rates, Q_i , and switch time, t^* , and thus can be applied whatever the configuration, size and productivity of the SMB unit in both linear and non-linear systems.

The modeling and simulation of SMB chromatographic processes is an important way to investigate the separation performance. In this study, direct SMB simulation approach, which takes into account the periodic switch of the injection and collection points, was used to simulate the SMB separation performance. The model was based on axially dispersed plug flow for the fluid and a linear mass transfer rate expression.

The differential mass balance equation over a slice of stationary column of SMB process is given as:

$$\frac{\partial c_i}{\partial t} = D_L \frac{\partial^2 c_i}{\partial z^2} - v \frac{\partial c_i}{\partial z} - \frac{1 - \varepsilon}{\varepsilon} \frac{\partial q_i}{\partial t} \quad (20)$$

The linear driving force approximation gives us

$$\frac{\partial q_i}{\partial t} = k(q_i^* - q_i) \quad (21)$$

With Danckwert's boundary conditions:

$$D_L \frac{\partial c_i}{\partial z}(z = 0, t) = -v[c_i(z = 0^-, t) - c_i(z = 0^+, t)] \quad (22)$$

$$\frac{\partial c_i}{\partial z}(z = L, t) = 0 \quad (23)$$

where q_i^* is the solid-phase concentration which is in equilibrium with the fluid phase concentration.

In the dimensionless form the equations are written as:

$$\frac{\partial Y_i}{\partial \tau} = \frac{1}{Pe} \frac{\partial^2 Y_i}{\partial Z^2} - \frac{\partial Y_i}{\partial Z} - FSt_i \cdot \left(\frac{q_{i,S}}{C_0} \right) (X_i^* - X_i) \quad (24)$$

$$\frac{\partial X_i}{\partial \tau} = St_i (X_i^* - X_i) \quad (25)$$

The boundary conditions convert to:

$$\frac{\partial Y_i}{\partial Z}(Z = 0, \tau) = -Pe[Y_i(Z = 0^-, \tau) - Y_i(Z = 0^+, \tau)] \quad (26)$$

$$\frac{\partial Y_i}{\partial Z}(Z = L, \tau) = 0 \quad (27)$$

where $Z = z/L$, $y_i = c_i/c_0$, $X_i^* = q_i^*/q_{i,S}$, $X_i = q_i/q_{i,S}$, $Pe = vL/D_L$, $\tau = vt/L$, $St = kL/v$, and $F = 1 - \varepsilon/\varepsilon$

Applying the technique of orthogonal collocation and neglecting the subscript i for shortness, we have:

$$\frac{dY(j)}{d\tau} = \frac{1}{Pe} \sum_{i=1}^{m+2} BX(j, i)Y(i) - \sum_{i=1}^{m+2} AX(j, i)Y(i) - FSt \left(\frac{q_S}{C_0} \right) (X^* - X) \quad (28)$$

$$\frac{dX}{d\tau} = St(X^* - X) \quad (29)$$

The boundary conditions become:

$$\sum_{i=1}^{m+2} AX(1, i)Y(i) = -Pe[Y(0) - Y(1)] \quad (30)$$

$$\sum_{i=1}^{m+2} AX(m+2, i)Y(i) = 0 \quad (31)$$

The boundary conditions can be rearranged and expanded to provide expressions for calculating $Y(1)$ and $Y(m+2)$.

From boundary condition 1 of Eq. (30):

$$Y(1) = \frac{-\left[PeY(0) + \sum_{i=2}^{m+2} AX(1, i)Y(i) \right]}{AX(1, 1) - Pe} \quad (32)$$

From boundary condition 2 of Eq. (31):

$$Y(m+2) = \frac{-\sum_{i=1}^{m+1} AX(m+2, i)Y(i)}{AX(m+2, m+2)} \quad (33)$$

At the inlet of the desorbent stream

$$Y(1) = 0 \quad (34)$$

At the inlet of the feed stream (column N)

$$Y(1)_{\text{Col}N} = \frac{Q_2 Y(m+2)_{\text{Col}N-1} + Q_F Y_F}{Q_3} \quad (35)$$

For all other columns

$$Y(1)_{\text{Col}N} = Y(m+2)_{\text{Col}N-1} \quad (36)$$

In binary (or pseudo-binary) SMB separation, each component in each column has two differential equations at each internal collocation point. In our study, there were eight columns in a 2-2-2-2 configuration (see Section 3). Eighteen (18) collocation points were used for each column, including those of the column inlet and outlet points. Therefore, there were $8 \times 2 \times 2 \times 18 = 576$ ordinary differential equations which can be solved by Gear's method. Using the IMSL integration routine IVPAG, the differential equations are solved and the steady-state concentration profiles can be calculated.

3. Experimental

3.1. Chemicals

HPLC-grade methanol was obtained from Fisher Scientific (Leics, UK). Glacial acetic acid and triethylamine were obtained from Merck (Germany). HPLC water was made in the laboratory using a Millipore ultra-pure water system. The racemate mixture of nadolol was purchased from Sigma (St. Louis, MO, USA). All purchased products are used without further purification.

Empty column (25 cm × 1 cm i.d. assembly was purchased from Phenomenex (USA). The columns were packed with perphenyl carbamoylated beta-cyclodextrin bonded onto silica gel using an Alltech pneumatic liquid pump (Alltech, USA) by slurry packing method. The silica gel was supplied by Hypersil (UK) with particle size of 15–25 μm. The eluent (desorbent) used was a binary mixture containing 80% aqueous buffer solution (1% TEAA, pH = 5.5) and 20% methanol. The feed solution was prepared by dissolving racemate of nadolol in the desorbent at concentration of 0.25 mg/ml. The eluent and feed solution were degassed in a model LC 60H ultrasonic bath before running the experiment.

3.2. SMB separation system

The SMB separation unit is open-looped and consists of eight columns (25 cm × 1 cm i.d.) arranged in a 2-2-2-2 configuration, i.e., two columns per section. Five flows (feed, eluent, extract, raffinate, and recycled eluent) are needed to handle in the SMB unit. The two inlet streams, i.e., feed and eluent, as well as two of the three outlet streams, i.e., extract and raffinate, are controlled by four HPLC pumps and thus leaving the recycled eluent stream free and determined by the overall material balance of the SMB unit. In particular, the feed solution is pumped in using a Shimadzu LC-10AT pump (Tokyo, Japan) and the eluent is pumped using a Perkin-Elmer series 200 LC pump which mixes the binary mixture of buffer solution and methanol at the desired composition. An online vacuum degasser (SUPELCO) degasses all the liquid being pumped into the system. The two outlet streams, i.e., the extract and raffinate, are controlled by two Jasco PU-1587 pumps. For cross-checking of product flow rate, the vessels containing the collected products are weighed on electronic balances (Mettler AE240).

Extra-column dead volume causes increases in retention time of the component to be separated and additional extra-column band broadening. This can be accounted and compensated in theory by the use of modified flow rate ratios in the frame of equilibrium theory [21] and in practice by minimizing the dead volume between columns of SMB unit. In this study, an eluent pump instead of a recycle pump (the recycle pump is fixed with respect to columns or zones of SMB) was used. This reduced the extra-column dead volume introduced by recycle pump. The compact design of

SMB setup produces an average extra-column dead volume of 0.6 ml per column, which account for approximate 3% of one column volume. Due to the small value of extra-column dead volume, the operating points are not shifted too much in the (m_2 , m_3) separation region compared with that considering the effect of extra-column dead volume.

The concentrations of the extract and raffinate streams were analyzed using Shimadzu SCL-10AVP chromatographic system. The samples of products were collected at the middle of the switch times at different cycle and switch times. An analytical column (25 cm × 0.46 cm i.d.) packed by perphenyl carbamoylated β-CD bonded onto 5 μm silica gel was used to analyze the concentration of samples based on calibration lines obtained previously from external standard nadolol solutions. The absorbance wavelength was set at 280 nm.

4. Results and discussions

4.1. Optimal and robust operation of SMB for ternary separation of nadolol

Equilibrium and kinetic parameters were essential for design and modeling of SMB process. These parameters for the separation of nadolol have been evaluated on the perphenyl carbamoylated β-CD bonded silica gel with particle sizes of 15 μm [13]. However, more than one column are needed (normally 8–16 columns are used) in practical applications of SMB, thus a great deal of packing materials are required. Besides, due to pressure limit of the whole system, the maximum back pressure of each single column is restricted to achieve stable operation and accurate controlling of products flow rates. So, for economic and operation considerations, usually larger particle size (e.g., in the range of 10–50 μm) of silica gel is used in the SMB operation. This is especially economical in the case when only specific application rather than general ones is required. In this study, perphenyl carbamoylated β-CD immobilized onto 15–25 μm silica gel were synthesized and packed into eight semi-preparative columns (25 cm × 1 cm i.d.). The bed voidage and axial mixing in the columns were determined by pulse chromatographic experiments using non-retained 1,3,5-tri-*tert*-butyl-benzene (TTBB) as the tracer. The average bed voidage and axial dispersion coefficients were found to be 0.47 and 0.0060v, respectively. The adsorption isotherm was evaluated on an analytical column (25 cm × 0.46 cm i.d.) packed with the same CSP and the equilibrium constants were found to be 5.34, 6.80 and 11.20 for (*SRS*)- and (*SSR*)-nadolol (considered as one component), (*RRS*)-nadolol and (*RSR*)-nadolol, respectively. They correspond to the first, second and third peaks of the elution chromatogram and are also represented by components 1–3, respectively, throughout the paper. Competitive Langmuir coefficients were evaluated by *h*-root method discussed elsewhere [22]. The b_i coefficients

were found to be 0.11, 1.72 and 8.85 for components 1–3, respectively.

As discussed early, one is mostly concerned with the projection of the four-dimensional space, m_j ($j = 1, \dots, 4$), onto (m_2, m_3) plane, i.e., the plane in the operating parameter space spanned by the flow rate ratios of the two key sections of the SMB unit. From Eqs. (1)–(3), different complete separation regions for ternary separation of nadolol was constructed in the (m_2, m_3) plane for both (1, 2) and (2, 3) separation regime based on equilibrium theory, as shown in Fig. 2. It is worth noting that for proper operation of SMB to obtain desired complete separation, adsorbent and fluid should be regenerated in sections 1 and 4, respectively, i.e., constraints of Eqs. (12) and (13) must be fulfilled. Attention should be paid that unlike the critical value of m_1 , critical value of m_4 is a function of feed concentration and operation conditions (i.e., m_2 and m_3). The critical value of m_4 ($m_4 = \omega_1^R$), coincides with the smallest root of Eq. (14) in the interval of $0 < \omega_1^R < a_1$. In the practical application, we obtained ω_1^R and thus $m_{4,cr}$ by trial and error method (e.g., simply by using MS Excel) instead of solving the complicated non-linear Eq. (14).

Provided that Eqs. (12) and (13) are fulfilled, it is useful to analyze different separation regions in the (m_2, m_3) plane by the concept of standing waves (or shocks), e.g., the regions around complete (2, 3) separation. In our separation of ternary mixture of nadolol to obtain enantiomer (RSR)-nadolol, components 1 and 2 should be conveyed upwards with fluid and collected in raffinate stream while component 3 ($p = C = 3$) be conveyed downwards with solid and collected in extract stream. Thus, rear flank of the simple wave transition through which component 2 is eluted should be standing in section 2 with zero propagating velocity. This is the smallest m_2 value to achieve the state (represented by line $c_n w_{n,p}$), further smaller m_2 could make the strongest component in raffinate (i.e., component 2) move downwards thus contaminate extract stream although purity of raffinate stream is still maintained (its recovery decreased), this region is named pure raffinate region. On the other hand, the shock transition of component 3, through which this component is adsorbed, is standing in section 3. This is the largest m_3 value to achieve the state (represented by line $w_{n,p} r_{n,p}$), further larger m_3 could make the weakest component in extract (i.e., component 3) move upwards thus contaminate raffinate stream although purity of extract stream is maintained, the

Table 1

Components (1–3) distribution in product streams in different separation regions of four-zone SMB

(n, p) regime	Separation regions	Extract	Raffinate
$n = 1, p = 2$	Complete separation	2, 3	1
	Pure raffinate	1–3	1
	Pure extract	2, 3	1, 2
$n = 2, p = 3$	Complete separation	3	1, 2
	Pure raffinate	2, 3	1, 2
	Pure extract	3	1–3

region is termed pure extract region. The optimal operating point is just the intersection of the two lines of $c_n w_{n,p}$ and $w_{n,p} r_{n,p}$, at this point the smallest m_2 value and the largest m_3 value to obtain the desired (2, 3) separation regime occur simultaneously, therefore the productivity of the unit is maximized. Besides, curve $r_{2,3} d_3$ represents the largest value of m_2 for the front flank of the component 3 to stand in section 2 to establish the required state. Further increasing of m_2 could also make the weakest component in extract (i.e., component 3) move upwards thus contaminate raffinate stream, thus one would also go to the pure extract region.

In Fig. 2, if one decreases m_2 and m_3 along operation line l (feed flow rate remains unchanged), one would undergo different regions of pure extract of (2, 3) separation regime, complete (2, 3) separation, pure raffinate of (2, 3) separation regime, complete (1, 2) separation and pure raffinate of (1, 2) separation regime. The components distributions in extract and raffinate streams are shown in Table 1. It is worth noting that the pure raffinate region of (2, 3) separation regime is identical to the pure extract region of (1, 2) separation regime. Several experimental runs were carried out around (2, 3) complete separation region and the results are shown in Table 2. It was found that the product purities are consistent with the corresponding regions. It should be noted that in separation of the ternary mixture of nadolol into component 3 in extract and components 1 and 2 in raffinate, components 1 and 2 are assumed to be one single component, so even 100% purity of raffinate stream is merely a binary mixture. Furthermore, when the difference of m_2 and m_3 increase (from run R to T), the separation performance of the unit such as yield and productivity increase. To find the possible optimal operation condition, one could operate SMB on different conditions along different

Table 2

Experimental results of SMB separation of nadolol in different separation regions

Run	Flow rate ratios				Switch time (t^*) (min)	Flow rates (ml/min)				Product purity (%)	
	m'_1	m'_2	m'_3	m'_4 (ω_1^R)		Q_1	Q_F	Q_R	Q_E	E	R
Q	13.44	9.55	10.02	4.44 (5.3321)	15.0	6.08	0.18	2.14	1.49	99.5	88.6
R	13.44	7.05	7.52	4.44 (5.3223)	15.0	6.08	0.18	1.18	2.45	99.5	99.8
S	13.44	6.05	6.52	4.42 (5.3057)	15.0	6.08	0.18	0.80	2.83	82.2	99.9
T	13.44	6.25	7.31	4.41 (5.2904)	15.0	6.08	0.41	1.11	2.76	99.4	99.8

operation lines, such as l and m in Fig. 2, and with the decreasing of m_2 and m_3 one would undergo different (2, 3) separation regions. The conditions that complete separation region were changed to either pure raffinate region or pure extract region correspond to real boundaries of complete separation region on the (m_2, m_3) plane. By connecting the corresponding points, one could obtain an approximate optimal operation point from the intersection point, which may be different from the theoretical one represented by $w_{2,3}$. This is due to possible perturbations in experimental operations, the limitation of equilibrium theory which neglects axial mixing and mass transfer resistances as well as the inaccuracies of parameters such as the competitive Langmuir isotherm and column total porosity.

4.2. Effect of non-linearity on the separation of SMB

For the four-zone SMB separation of ternary mixture of nadolol, effects of non-linearity on the separation performances were also investigated, which includes overall feed concentration and composition of the components to be separated.

The boundaries of complete (1, 2) and (2, 3) separation region for different feed concentrations were calculated simply by using Eqs. (1)–(3), with fixed feed composition, i.e., mole fraction of components 1, 2 and 3 is 0.5, 0.25, 0.25, respectively. Fig. 3 showed that both linear and non-linear complete separation region for (2, 3) separation regime is larger than that for (1, 2) separation regime, because $a_3 - a_2$ is greater than $a_2 - a_1$. This explained the reason why it is easier to split a ternary mixture between components with larger equilibrium constant difference (e.g., between components 2 and 3 of nadolol) than that with smaller difference (e.g., between components 1 and 2) in SMB separation. It was found that with increasing feed concentrations, the

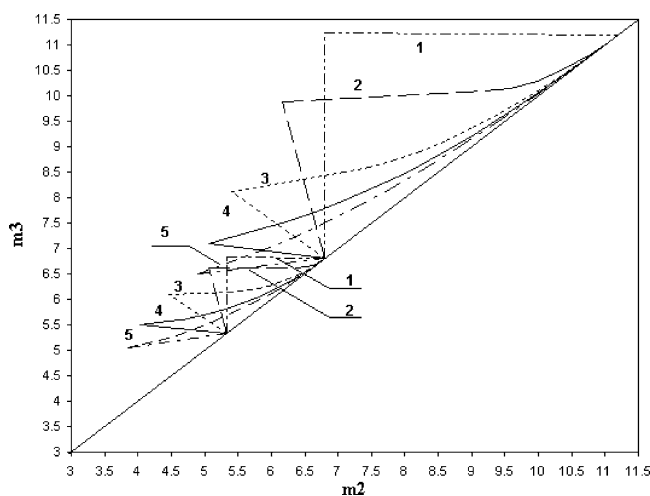


Fig. 3. Effect of changing feed concentrations on complete separation region for separation of ternary mixture of nadolol by four-zone SMB (1: linear system, $c = 0.0001$ mg/ml; 2: $c = 0.05$ mg/ml; 3: $c = 0.15$ mg/ml; 4: $c = 0.25$ mg/ml; 5: $c = 0.35$ mg/ml).

optimal points of $w_{n,p}r_{n,p}$ moved towards the lower left corner of the plane and the complete (1, 2) and (2, 3) separation region become smaller and sharper with a long tail (curve $r_{n,p}d_p$). In other words, the complete separation regions gained increasing non-linear characters, which required that flow rate ratios of m_2 and m_3 must be decreased to achieve complete separation. It is also worth pointing out that larger feed concentrations imply smaller upper bounds on m_4 (i.e., ω_1^R according to Eq. (14)), which means smaller flow rate ratio in section 4 are required to avoid more concentrated fronts of the relative species reaching the end of this section between two successive switches. This effect is a consequence of the property of favorable Langmuir isotherm, for which the propagation velocity of concentration waves increase with increasing feed concentration.

The effect of feed composition on SMB separation performances was also analyzed. In Fig. 4, both (1, 2) and (2, 3) complete separation regions were obtained for three cases whose mole fraction of the strongest component (i.e., component 3) is 0.25, 0.33 and 0.50, respectively. In particular, feed mole fractions of the three components are 0.5:0.25:0.25 (representing separation of nadolol in this study), 0.33:0.33:0.33 (equal composition of ternary mixture) and 0.25:0.25:0.5, respectively. It can be readily observed that although the intersection between (1, 2) and (2, 3) complete separation regions and the diagonal remain the same (like that in Fig. 3), the optimal points move downwards to the left, yielding a marked distortion of the complete separation regions. The regions become smaller and sharper as the mole fraction of the strongest component increases. This behavior is assumed to be due to the non-adsorbable nature of the desorbent [18]. It is thus obvious that decreasing mole fraction of the strongest component in the feed mixture could result in a larger and wider

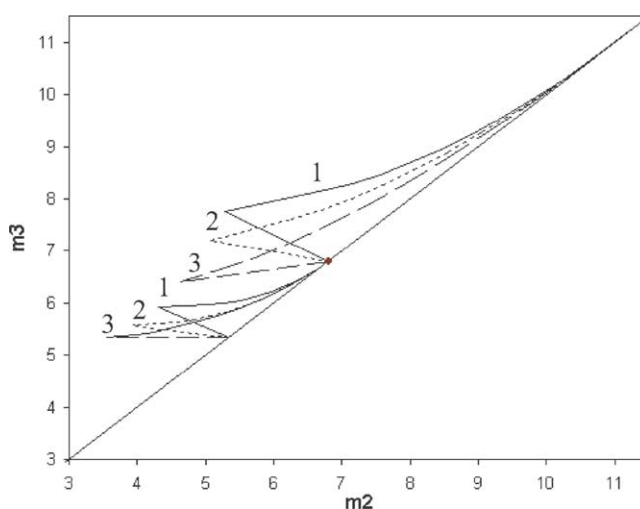


Fig. 4. Effect of changing feed composition on complete separation region for separation of ternary mixture by four-zone SMB (total feed concentration is 0.1787 mg/ml and compositions of components A–C for cases 1–3 are: (1) 0.25:0.25:0.5; (2) 0.33:0.33:0.33; and (3) 0.5:0.25:0.25, respectively).

complete separation region as well as a higher productivity possibly achieved by the SMB unit.

4.3. Simulation of pseudo-binary separation of nadolol

Boundaries of complete separation region in the (m_2, m_3) plane have been determined for both (1, 2) and (2, 3) separation regime. This is very useful at the stage of design and operation of SMB unit, especially for the separation of ternary mixture of nadolol if different separation requirements such as (1, 2) and (2, 3) complete separations are raised. In our study of separation of nadolol into its two components by four-zone SMB, the most strongly adsorbed component 3 ((RSR)-enantiomer of nadolol) should be produced in extract product and binary mixture of components 1 and 2 should be obtained in raffinate stream. In particular, component I was used to refer to binary mixture of components 1 and 2 (which are assumed to be one single component) and component II refers to component 3. Thus, the ternary mixture of nadolol can be reduced into an equivalent pseudo-binary mixture constituted only of the weak-key (component 2) and strong-key (component 3) components. The equilibrium parameters of components I and II can be expressed from the corresponding parameters of the original ternary system and concentration of the weak-key in the feed stream can be taken equal to the sum of the concentrations of components 1 and 2:

$$a_{\text{I}} = a_2 = 6.8, \quad b_{\text{I}} = b_2 = 1.72 \quad (37)$$

$$a_{\text{II}} = a_3 = 11.2, \quad b_{\text{II}} = b_3 = 8.85 \quad (38)$$

$$c_{\text{I}} = c_1 + c_2 \quad (39)$$

$$c_{\text{II}} = c_3 \quad (40)$$

The pseudo-binary separation defined by Eqs. (37)–(40) was believed to be as difficult as, or in general more difficult than the separation determined from Langmuir isotherms of the three components and their corresponding concentrations in the feed [8]. However, the validity and extent of conservative of the separation region obtained from the “shortcut” method compared with the “true” separation region has not been discussed in a quantitative way and this deserves to be investigated for practical applications. In Fig. 5, boundaries represented by curve a were determined from all three components in the ternary mixture while boundaries of curve b was obtained from the shortcut method of pseudo-binary separation. It was found that the complete separation region obtained from the shortcut method is a subset of the true complete separation region and the optimal separation conditions obtained differed slightly from the “true” separation. It is also worth noting that run T is located inside the complete separation regions of both cases. Thus, modeling and simulation of the pseudo-binary separation can be conducted on the basis of the shortcut method.

The cyclic steady-state concentration profile for operation at run T is shown in Fig. 6. The experimental results were

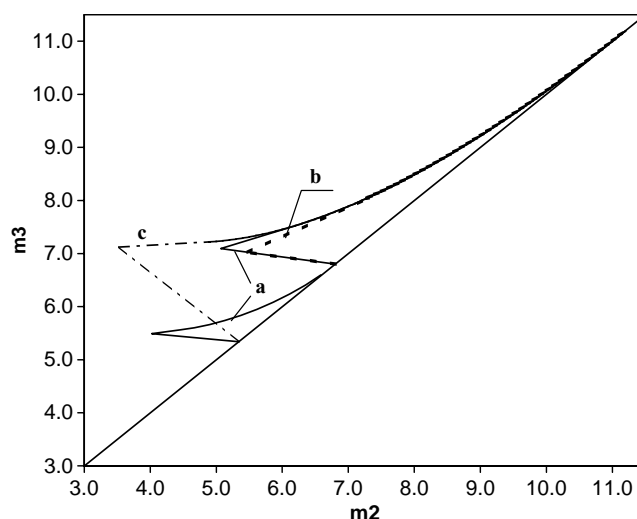


Fig. 5. Complete separation regions of the four-zone SMB for separation of nadolol. (a) Ternary separation determined from three components in the ternary mixture, (b) Pseudo-binary separation using component 2 as the weak-key, (c) Pseudo-binary separation using component 1 as the weak-key, which covers (1, 2) and (2, 3) complete separation regime.

obtained by sampling the outlet solution at column 8 for eight consecutive switches. The samples collected during the first switch in a cycle represent the column outlet concentration of column 8 and the second switch, column 7 and so on. The collections for each switch were performed at the mid-time within the switches. The progression of the concentration profiles within a switch interval for the eight columns was compared with the values calculated from the mathematical model. Sixteen internal collocation points were chosen in the orthogonal collocation method after taking consideration of the accuracy of the simulation results, system stability and the optimum usage of computer time. Generally, good agreement between the theoretical and experimental profiles was observed.

It is worth noting that some experimental results varied from theoretical profiles. This could be due to different

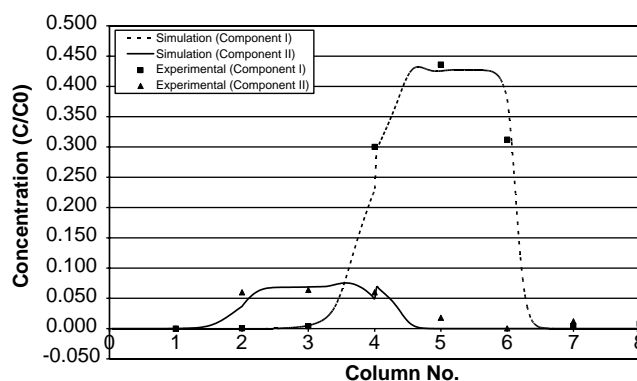


Fig. 6. Steady-state concentration distribution profile in the four-zone SMB (Lines and points represent simulated and experimental results, respectively). Operation conditions at run T: $t^* = 15$ min, $Q_1 = 6.08$ ml/min, $Q_f = 0.41$ ml/min, $Q_R = 1.11$ ml/min, and $Q_E = 2.76$ ml/min.

chemico-physical parameters of columns in the SMB unit, which is possibly caused by different batches of synthesized adsorbents and the difficulty of obtaining reproducible columns by conventional slurry packing method for larger diameter columns. The disagreement could also be due to the difficulty of controlling flow rates accurately in the SMB experimental studies. Besides, sample collections from column 8 during steady state could deteriorate the operation and cause experimental errors.

It should be pointed out that due to diffused and partially resolved elution peaks between the first and second component, it was difficult to obtain accurate kinetic parameters. Besides particle size of the silica gel to which CSP was immobilized, mass transfer coefficient may also be influenced by solute concentration, fluid velocity and the presence of the other component. Since it is well believed that gross features of the dynamic behavior of the SMB system were mainly determined by the equilibrium relationship rather than by kinetic coefficients, mass transfer coefficients obtained from the same CSP immobilized onto 15 μm silica gel were applied in the simulation. The mass transfer coefficients for components I and II were approximated to be 846 and 106 min^{-1} , respectively, which were determined from moment analysis of the response peaks in a previous study [13]. In our simulation, 5- and 10-fold decrease of the mass transfer coefficients (smaller values are expected for larger particles with wider size distribution) were also applied, which only affect simulation result in an insignificant manner.

It was observed from our simulation study that the theoretical profiles were much more sensitive to the equilibrium isotherm than to the accurate determination of mass transfer resistances. In general, the cyclic steady-state profiles calculated from the model used in this study are in good agreement with the experimental values and the model is adequate in simulating the SMB separation performance.

5. Conclusions

Four-zone SMB was employed to separate the target enantiomer of nadolol from its ternary mixture in non-linear region. Provided that adsorbent and fluid be regenerated properly in sections 1 and 4, respectively, different regions of (2, 3) and (1, 2) complete separation regime were determined in the (m_2, m_3) region. A practical way of obtaining the approximate optimal operation condition from experimental results was proposed. The effect of non-linearity including the overall feed concentration and component composition on the separation performances was investigated and the shape and location of the corresponding complete separation region were examined thoroughly.

A direct simulation approach has been used to simulate the operation and performance of a simulated moving bed process for separation of ternary mixture of nadolol in the four-zone SMB. The simulation of the pseudo-binary

separation was conducted on the basis of a shortcut method constituted only of the weak-key and strong-key components. The performance of the cyclic steady-state behavior of the separation unit is predicted reasonably well. The parameters determined by pulse experiments and moment analysis seem to be adequate in simulating SMB cyclic steady-state behavior. Although the model does not account for the variation in mass transfer coefficient and dead volume introduced by the tubing between columns, simulation results show that the separation performance is more sensitive to the accurate determination of the adsorption isotherms than that of mass transfer coefficient.

Acknowledgements

Financial support from National University of Singapore (NUS) is gratefully acknowledged. Thanks are also due to Y.X. Wu and Z.Y. Zhang for helpful discussions.

Nomenclature

a_i	intrinsic affinity coefficients (dimensionless)
b_i	Langmuir competitive interference coefficient (ml/mg)
c_i	mobile-phase concentration based on fluid volume (mg/ml)
c_i^F	feed concentration (mg/ml)
D_L	axial dispersion coefficient (cm^2/s)
F	phase ratio, equal to $(1 - \varepsilon)/\varepsilon$
k	lumped mass transfer coefficient (s^{-1} or min^{-1})
L	column length (cm)
m_j	fluid-phase flow rate over solid phase flow rate in section j of TCC and SMB unit
$m_{1,\text{cr}}$	critical flow rate ratio in section 1 of SMB, $m_{1,\text{cr}} = a_3$
$m_{4,\text{cr}}$	critical flow rate ratio in section 4 of SMB, $0 < m_{4,\text{cr}} < a_1$
Pe	Peclet number, vL/D_L
q_i	concentration of component i on stationary phase (mg/ml)
$q_{i,S}$	adsorbed phase saturation concentration, a_i/b_i
q_i^*	equilibrium concentration of component i on stationary phase (mg/ml)
Q_F	feed flow rate fed to SMB process
Q_j	liquid phase flow rate in section j of TCC or SMB process
Q_S	solid-phase flow rate in both TCC and SMB processes
St	Stanton number, kl/v
t	time coordinate
t^*	switching time in SMB process (min)
v_L	interstitial fluid velocity of the fluid phase in SMB process
v_S	solid velocity in TCC process

V	column volume
X_i	dimensionless solid-phase concentration, $q_i/q_{i,S}$
X_i^*	dimensionless solid-phase equilibrium concentration, $q_i^*/q_{i,S}$
Y_i	dimensionless concentration, c_i/c_0
z	space coordinate
Z	dimensionless distance, z/L

Greek symbols

ε	bed voidage
ε^*	total porosity of column
τ	dimensionless time coordinates ($\tau = vt/L$)
ω	components of Ω vectors defined elsewhere [9]

Subscripts

ColN	column number N in SMB unit
D	desorbent
F	feed
L	liquid phase
n	strong-key component in raffinate stream
p	weak-key component in extract stream
S	solid phase
1	the first eluted component of nadolol racemic mixture (component 1)
2	the second eluted component of nadolol racemic mixture (component 2)
3	the third eluted component of nadolol racemic mixture (component 3)
I	the binary mixture of components 1 and 2 (assumed to be one single component) in the four-zone SMB separation of nadolol
II	the third eluted component of nadolol racemic mixture

Superscripts

SMB	simulated moving bed chromatography
TCC	true counter-current chromatography

F	SMB feed stream
R	SMB raffinate product references

References

- [1] A.M. Krstulovic, J. Chromatogr. 488 (1989) 53.
- [2] S. Ahuja, in: H.Y. Aboul-Enein, I.W. Wainer (Eds.), *The Impact of Stereochemistry in Drug Development and Use*, John Wiley and Sons, New York, 1997, p. 287.
- [3] Anon. Chirality 4 (1992) 338.
- [4] E. Francotte, P. Richert, M. Mazzotti, M. Morbidelli, J. Chromatogr. A 796 (1998) 239.
- [5] S.L. Pais, M.J. Loureiro, A.E. Rodrigues, Chem. Eng. Sci. 52 (1997) 245.
- [6] S. Khattabi, D.E. Cherrak, K. Muhlbachler, G. Guiochon, J. Chromatogr. A 877 (2000) 95.
- [7] C.B. Ching, B.G. Lim, E.J.D. Lee, S.C. Ng, J. Chromatogr. 634 (1993) 215.
- [8] M. Mazzotti, G. Storti, M. Morbidelli, AIChE J. 40 (1994) 1825.
- [9] C. Migliorini, M. Mazzotti, M. Morbidelli, Sep. Purif. Technol. 20 (2000) 79.
- [10] V. Mata, A.E. Rodrigues, J. Chromatogr. A 939 (2001) 23.
- [11] http://www.organo.co.jp/technology/hisepa/en_hisepa/newjo/jo1.html.
- [12] D.C.S. Azevedo, A.E. Rodrigues, Carbohydrate Separation From Cashew Apple Juice: Experimental Data in SMB, AIChE Meeting in Indianapolis, 2002.
- [13] X. Wang, C.B. Ching, Sep. Sci. Technol. 37 (2002) 2567.
- [14] G. Storti, M. Masi, S. Carra, Chem. Eng. Sci. 44 (1989) 1329.
- [15] G. Storti, M. Mazzotti, M. Morbidelli, S. Carra, AIChE J. 39 (1993) 471.
- [16] G. Storti, M. Mazzotti, M. Morbidelli, R. Bachiocci, Ind. Eng. Chem. Res. 34 (1995) 288.
- [17] M. Mazzotti, G. Storti, M. Morbidelli, AIChE J. 42 (1996) 2784.
- [18] M. Mazzotti, G. Storti, M. Morbidelli, AIChE J. 43 (1997) 64.
- [19] M. Mazzotti, G. Storti, M. Morbidelli, J. Chromatogr. A 769 (1997) 3.
- [20] D.M. Ruthven, C.B. Ching, Chem. Eng. Sci. 44 (1989) 1011.
- [21] C. Migliorini, M. Mazzotti, M. Morbidelli, AIChE J. 45 (1999) 1411.
- [22] X. Wang, C.B. Ching, Ind. Eng. Chem. Res. 42 (2003) 6171.